Strojniški vestnik - Journal of Mechanical Engineering 51(2005)11, 692-710
UDK - UDC 532.528:532.542
Izvirni znanstveni članek - Original scientific paper (1.01)

Diskretni plinski kavitacijski model z upoštevanjem vpliva nestalnega kapljevinskega trenja v cevi

A Discrete Gas-Cavity Model that Considers the Frictional Effects of Unsteady Pipe Flow

Anton Bergant - Uroš Karadžić - John Vítkovský - Igor Vušanović - Angus R. Simpson

Prehodni kavitacijski tok pare v cevi vzbudi padec tlaka na parni tlak kapljevine. Podan je kratek oris metode karakteristik, temu slede osnove nestalnega kapljevinskega trenja in prehodnega kavitacijskega toka v cevi. Glavni cilj tega prispevka je predstavitev novega plinskega kavitacijskega modela (DPKM) z upoštevanjem vplivov nestalnega trenja. Rezultati izračuna so primerjani z rezultati meritev v laboratoriju. Upoštevanje nestalnega trenja v DPKM da bolj natančne računske rezultate.

(Ključne besede: sistemi cevni, udari vodni, tok kavitacijski, modeli kavitacijski diskretni plinski, trenje nestalno)

Transient, vaporous, cavitating pipe flow occurs when the pressure drops to the liquid's vapour pressure. A brief description of the method of the characteristics and fundamentals of unsteady pipe-flow friction and transient, cavitating pipe flow are given. The main objective of this paper is to present a novel, discrete gas-cavity model (DGCM) with a consideration of unsteady frictional effects. The numerical results are compared with the results from laboratory measurements. The inclusion of unsteady friction into the DGCM significantly improves the numerical results.

(Keywords: piping systems, water hammer, cavitating flow, discrete gas cavity models, unsteady friction)

0 UVOD

Hidravlični cevni sistemi morajo varno delovati v širokem pasu obratovalnih režimov. Vodni udar vzbudi nihanje tlaka v cevnih sistemih, spremembo vrtilne frekvence (narastek, nasprotno vrtenje) v hidravličnih strojih in nihanje gladine vode v izravnalnikih. Prehodni pojavi v ceveh lahko povzročijo zadosten padec tlaka, ki vodi do prekinitve homogenosti in kontinuitete kapljevine (pretrganje kapljevinskega stebra). Neželeni vplivi vodnega udara lahko ustavijo obratovanje hidravličnih sistemov (hidroelektrarna, črpalni sistem) in poškodujejo elemente sistema; na primer zrušitev cevovoda. Obremenitve vodnega udara v dopustnih mejah lahko dosežemo z ustreznim krmiljenjem obratovalnih režimov, vgradnjo elementov za blažitev vodnega udara ali prerazporeditvijo elementov cevnega sistema ([1] in [2]). Umerjanje in nadzor

0 INTRODUCTION

Hydraulic piping systems should work safely over a broad range of operating regimes. Water hammer induces pressure fluctuations in piping systems, rotational speed variations (overspeed, reverse rotation) in hydraulic machinery or water-level oscillations in surge tanks. Transients in pipelines can cause a drop in pressure large enough to break the liquid's homogeneity and continuity (liquid column separation). Undesirable water-hammer effects can disturb the overall operation of hydraulic systems (hydroelectric power plant, pumping system) and damage system components; for example, pipe rupture can occur. Water-hammer loads can be kept within the prescribed limits by the adequate control of the operational regimes, the installation of surge-control devices or the redesign of the original pipeline layout ([1] and [2]). The calibration and monitor-

hidravličnih sistemov narekujeta potrebo po globljem poznavanju fizike tlačnih valov [3].

Prvi del prispevka obravnava matematična orodja za modeliranje nestalnega kapljevinskega trenja in prehodnega parnega kavitacijskega toka (pretrganje kapljevinskega stebra). Premena enačb nestalnega toka v cevi z uporabo metode karakteristik da osnove algoritma za vodni udar. V deltoidno mrežo metode karakteristik je vgrajen konvolucijski model nestalnega trenja z uporabo zmogljivih računskih orodij [4]. Vgradnja diskretnih kavitacij v model vodnega udara da diskretni kavitacijski model ([2] in [5]). V prispevku je podan nov diskretni plinski kavitacijski model (DPKM) z upoštevanjem vpliva nestalnega kapljevinskega trenja v cevi. Podan je kratek oris preizkusne postaje za meritev vodnega udara. V zaključnem delu prispevka so podani številni primeri, iz katerih izhaja, da upoštevanje nestalnega kapljevinskega trenja v DPKM pomembno vpliva na napoved tlačnih valov v preprostem cevnem sistemu z ventilom.

1 TEORETIČNI MODEL

Vodni udar popisuje potovanje tlačnih valov v ceveh s kapljevino. Nestalni tok v cevi popišemo s kontinuitetno in gibalno enačbo [2]:

$$\frac{\partial H}{\partial t}+V\frac{\partial H}{\partial x}-V\sin\theta+\frac{a^2}{g}\frac{\partial V}{\partial x}=0 \tag{1}$$

$$g\frac{\partial H}{\partial x}+\frac{\partial V}{\partial t}+V\frac{\partial V}{\partial x}+f\frac{V|V|}{2D}=0 \tag{2}.$$

Naj omenimo, da so vse označbe definirane v poglavju 6. Postavimo tok v eni razsežnosti (po prerezu povprečena hitrost in tlak), tlak večji od parnega tlaka kapljevine, linearen elastični odziv stene cevi in kapljevine, nestalno trenje kapljevine nadomeščamo s stalnim, zanemarljivo količino prostih plinskih kavitacij v kapljevini in šibko interakcijo med kapljevino in ograde. Konvektivni členi $V(\partial H/\partial x)$, $V(\partial V/\partial x)$ in $V\sin\theta$ so majhni v primerjavi s preostalimi členi in jih v inženirski uporabi lahko zanemarimo ([1] in [2]). Z vpeljavo pretoka $Q = VA$ namesto povprečne pretočne hitrosti V se poenostavljeni sistem enačb (1) in (2) glasi:

ing of hydraulic systems requires a detailed knowledge of water-hammer waveforms [3].

The first part of the paper deals with mathematical tools for modeling unsteady pipe-flow friction and transient vaporous cavitation (liquid column separation). The method of characteristics transformation of the unsteady pipe-flow equations gives the water-hammer solution procedure. A convolution-based unsteady friction model using state-of-the-art numerical tools [4] is explicitly incorporated into the staggered grid of the method of characteristics. Incorporating discrete cavities into the water-hammer model leads to the discrete-cavity model ([2] and [5]). A novel discrete gas-cavity model (DGCM) with consideration of the unsteady pipe-flow friction effects is presented in the paper. The experimental apparatus for measurements of the water-hammer pressure waves is briefly described. The paper concludes with a number of case studies showing how the inclusion of unsteady friction into the DGCM significantly affects the pressure traces in a simple reservoir-pipeline-valve system.

1 THEORETICAL MODEL

Water hammer is the transmission of pressure waves in liquid-filled pipelines. Unsteady pipe flow is described by the continuity equation and the equation of motion [2]:

Note that all the symbols are defined in Section 6. The flow in the pipe is assumed to be one-dimensional (cross-sectional averaged velocity and pressure distributions), the pressure is greater than the liquid vapour pressure, the pipe wall and the liquid behave linearly elastically, unsteady friction losses are approximated as steady friction losses, the amount of free gas in the liquid is negligible and the fluid-structure coupling is weak. For most engineering applications, the transport terms $V(\partial H/\partial x)$, $V(\partial V/\partial x)$ and $V\sin\theta$, are very small compared to the other terms and can be neglected ([1] and [2]). A simplified form of Eqs. (1) and (2) using the discharge $Q=VA$ instead of the flow velocity V is:

$$\frac{\partial H}{\partial t}+\frac{a^2}{gA}\frac{\partial Q}{\partial x}=0 \tag{3}$$

$$\frac{\partial H}{\partial x}+\frac{1}{gA}\frac{\partial Q}{\partial t}+f\frac{Q|Q|}{2gDA^2}=0 \tag{4}.$$

Premena poenostavljenih enačb (3) in (4) z metodo karakteristik (MK) da združljivostne enačbe vodnega udara, ki veljajo vzdolž karakterističnih krivulj. Združljivostne enačbe v koračni obliki so numerično stabilne razen v primeru velikih izgub zaradi trenja in redke računske mreže. Obravnavane enačbe, zapisane za računsko točko *i* (sl. 1), se glase [2]:

- vzdolž C^+ karakteristike ($\Delta x/\Delta t = a$)

$$H_{i,t} - H_{i-1,t-\Delta t} + \frac{a}{gA}\left((Q_u)_{i,t} - (Q_d)_{i-1,t-\Delta t}\right) + \frac{f\Delta x}{2gDA^2}(Q_u)_{i,t}\left|(Q_d)_{i-1,t-\Delta t}\right| = 0 \quad (5),$$

- vzdolž C^- karakteristike ($\Delta x/\Delta t = -a$)

$$H_{i,t} - H_{i+1,t-\Delta t} - \frac{a}{gA}\left((Q_d)_{i,t} - (Q_u)_{i+1,t-\Delta t}\right) - \frac{f\Delta x}{2gDA^2}(Q_d)_{i,t}\left|(Q_u)_{i+1,t-\Delta t}\right| = 0 \quad (6).$$

V primeru vodnega udara sta pretok na navzgornjem koncu računske točke *i* ($(Q_u)_i$) in pretok na navzdolnjem koncu točke ($(Q_d)_i$) enaka (nestalni kapljevinski tok). Na robu (rezervoar, ventil) enačba robnega pogoja nadomesti eno od združljivostnih enačb vodnega udara. V tem prispevku bomo uporabili deltoidno mrežo metode karakteristik [2].

1.1 Nestalno kapljevinsko trenje v cevi

V algoritmih za vodni udar običajno uporabimo stalni ali navidezno stalni člen trenja. Ta

The method of characteristics (MOC) transformation of the simplified equations (3) and (4) produces the water-hammer compatibility equations, which are valid along the characteristics lines. The compatibility equations in finite-difference form are numerically stable unless the friction is large and the computational grid is coarse and, when written for a computational section *i* (Fig. 1), are [2]

- along the C^+ characteristic line ($\Delta x/\Delta t = a$)

- along the C^- characteristic line ($\Delta x/\Delta t = -a$)

The discharge at the upstream side of the computational section *i* ($(Q_u)_i$) and the discharge at the downstream side of the section ($(Q_d)_i$) are identical for the water-hammer case (unsteady liquid flow). At a boundary (reservoir, valve), a device-specific equation replaces one of the water-hammer compatibility equations. The staggered grid in applying the method of characteristics [2] is used in this paper.

1.1 Unsteady Pipe Flow Friction

Traditionally, the steady or quasi-steady friction terms are incorporated into the water-hammer

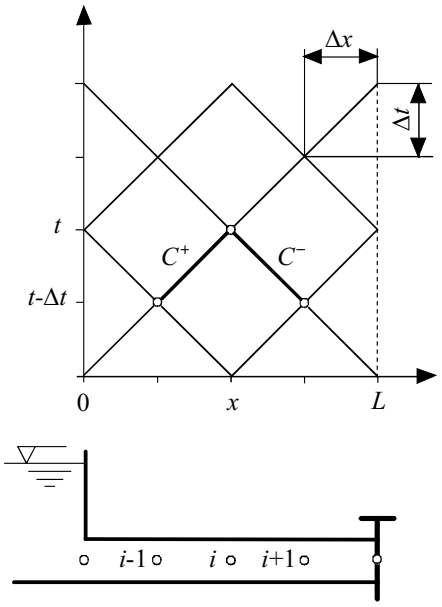

Sl. 1. *Deltoidna mreža metode karakteristik za sistem hram - cevovod - ventil*
Fig. 1. *The method of characteristics staggered grid for a reservoir-pipe-valve system*

postavka velja za počasne prehode, pri katerih so strižne sile navidezno stalne. Uporaba navidezno stalnega modela trenja za hitre prehode da, kakor so pokazale primerjave med rezultati izračuna in meritev ([6] do [8]), znatna odstopanja v dušenju, obliki in času poteka tlačnih valov. Koeficient trenja, zapisan neposredno v enačbah (5) in (6), lahko izrazimo kot vsoto navidezno stalnega dela f_q in nestalnega dela f_u [9]:

algorithms. This assumption is satisfactory for slow transients where the wall shear stress has a quasi-steady behaviour. Previous investigations using the quasi-steady friction approximation for rapid transients ([6] to [8]) showed significant discrepancies in the attenuation, the shape and the timing of the pressure traces when computational results were compared with measurements. The friction factor, explicitly used in Eqs. (5) and (6), can be expressed as the sum of the quasi-steady part f_q and the unsteady part f_u [9]:

$$f = f_q + f_u \tag{7}.$$

Navidezno stalni koeficient trenja f_q je odvisen od Reynoldsovega števila in relativne hrapavosti cevi. V literaturi so predlagani številni modeli nestalnega trenja, ki jih delimo na enorazsežne (1D) in dvorazsežne (2D) modele. V 1D modelih približamo dejanski 2D prečni profil hitrosti in ustrezajoče izgube trenja. Z 2D modeli računamo dejanski prečni profil hitrosti med prehodnim pojavom. Modele trenja lahko razporedimo v šest skupin [7]:

1) člen trenja je odvisen od trenutne povprečne hitrosti V,
2) člen trenja je odvisen od trenutne povprečne hitrosti V in trenutnega krajevnega pospeška $\partial V/\partial t$,
3) člen trenja je odvisen od trenutne povprečne hitrosti V, trenutnega krajevnega pospeška $\partial V/\partial t$ in trenutnega konvektivnega pospeška $a\partial V/\partial x$ (Brunonejev model),
4) člen trenja je odvisen od trenutne povprečne hitrosti V in difuzije $\partial^2 V/\partial x^2$,
5) člen trenja je odvisen od trenutne povprečne hitrosti V in uteži za hitrostne spremembe v preteklosti $W(\tau)$ (konvolucijski model),
6) člen trenja je odvisen od trenutne porazdelitve hitrosti po prerezu (2D modeli).

V prispevku bomo obravnavali konvolucijski model nestalnega trenja ([4], [10] do [12]).

The quasi-steady friction factor, f_q, depends on the Reynolds number and the relative pipe roughness. A number of unsteady-friction models have been proposed in the literature including one-dimensional (1D) and two-dimensional (2D) models. The 1D models approximate the actual 2D cross-sectional velocity profile and the corresponding viscous losses in different ways. The 2D models compute the actual cross-sectional velocity profile continuously during the water-hammer event. The friction term can be classified into six groups [7]:

1) The friction term is dependent on instantaneous mean flow velocity, V,
2) The friction term is dependent on instantaneous mean flow velocity, V, and the instantaneous local acceleration, $\partial V/\partial t$,
3) The friction term is dependent on the instantaneous mean flow velocity, V, the instantaneous local acceleration, $\partial V/\partial t$, and the instantaneous convective acceleration, $a\partial V/\partial x$ (Brunone's model),
4) The friction term is dependent on the instantaneous mean flow velocity, V, and the diffusion, $\partial^2 V/\partial x^2$,
5) The friction term is dependent on the instantaneous mean flow velocity, V, and the weights for past velocity changes, $W(\tau)$ (convolution-based model),
6) The friction term is based on the cross-sectional distribution of instantaneous flow velocity (2D models).

This paper deals with the convolution-based unsteady-friction model ([4], [10] to [12]).

1.2 Prehodni kavitacijski tok

Kavitacijski tok v cevi se pojavi pri nizkih tlakih med prehodnimi pojavi. Prehodna kavitacija znatno vpliva na obliko tlačnega vala. Enačbe vodnega udara postavljene za enofazni prehodni tok, ne veljajo za dvofazni prehodni tok. Prehodna kavitacija v ceveh se pojavi v dveh

1.2 Transient Cavitating Pipe Flow

Cavitating pipe flow usually occurs as a result of low pressures during a transient event. Transient cavitation significantly changes the water-hammer waveform. Water-hammer equations developed for a one-phase liquid are not valid for the two-phase transient fluid flow. There are two basic types of

oblikah ([2] in [3]):
1) enokomponentni dvofazni tok (parna kavitacija, pretrganje stebra),
2) dvokomponentni dvofazni tok (plinska kavitacija, prost plin v kapljevinskem toku).

V prispevku obravnavamo parno kavitacijo v ceveh. Kavitacija se lahko pojavi kot krajevna kavitacija z velikim kavitacijskim razmernikom - kavitacija na robu ali visokem kolenu vzdolž cevi, ali kot nepretrgani kavitacijski tok z majhnim kavitacijskim razmernikom - enakomerno porazdeljeni mehurčki v kapljevini.

Parna kavitacija v ceveh se pojavi, ko se tlak kapljevine zniža na parni tlak kapljevine. Postavimo zanemarljivo majhno količino prostega in/ali izločenega plina v kapljevini. Ta postavka velja v večini industrijskih cevnih sistemov. Tlačni val v cevi potuje s stalno hitrostjo pri tlaku, večjem od parnega tlaka kapljevine. Tlačni valovi ne obstajajo v področju nepretrganega parnega kavitacijskega toka. Nezmožnost potovanja tlačnega vala v področju nepretrganega parnega toka je karakteristična ločnica med parno in plinsko kavitacijo. Razviti so bili številni modeli za popis parne kavitacije, to so diskretni parni kavitacijski model (DPAKM), diskretni plinski kavitacijski model (DPKM) z upoštevanjem majhnega plinskega razmernika ($\alpha_g \leq 10^{-7}$) in kombinirani parni kavitacijski model ([2] in [5]). Diskretni plinski kavitacijski model je preprost in daje natančne rezultate v širokem pasu obratovanja sistema [13]. V prispevku podajamo nov DPKM z upoštevanjem nestalnega kapljevinskega trenja v cevi.

2 DISKRETNI PLINSKI KAVITACIJSKI MODEL Z UPOŠTEVANJEM NESTALNEGA TRENJA

Diskretni plinski kavitacijski model (DPKM) dopušča plinske kavitacije v računskih točkah numerične mreže metode karakteristik. V cevnih odsekih med numeričnimi točkami obstaja kapljevina, kjer potujejo udarni valovi s stalno hitrostjo a. Diskretno plinsko kavitacijo popišemo z združljivostnima enačbama vodnega udara (5) in (6), kontinuitetno enačbo za prostornino plinske kavitacije in plinsko enačbo [14]. V računski točki deltoidne mreže metode karakteristik se kontinuitetna enačba za prostornino plinske kavitacije in plinska enačba glasita:
- kontinuitetna enačba za prostornino plinske kavitacije

transient cavitating flow in pipelines ([2] and [3]):
1) One-component two-phase transient flow (vaporous cavitation, column separation),
2) Two-component two-phase transient flow (gaseous cavitation, free gas in liquid flow).

This paper deals with vaporous cavitating pipe flow. Cavitation can occur as localized cavitation with a large void fraction, such as when a cavity forms at a boundary or at a high point along the pipeline, or as distributed cavitation with a small void fraction, such as when cavity bubbles are distributed homogeneously in a liquid.

Vaporous cavitation occurs in pipelines when the liquid pressure drops to the vapour pressure of the liquid. The amount of free and/or released gas in the liquid is assumed to be small. This is usually the case in most industrial piping systems. The water-hammer wave propagates at a constant speed as long as the pressure is above the vapour pressure. Pressure waves do not propagate through an established mixture of liquid and vapour bubbles. The inability of pressure waves to propagate through a distributed vaporous cavitation zone is a major feature distinguishing the flow with vaporous cavitation from the flow with gaseous cavitation. A number of numerical models have been developed to describe vaporous cavitation, including the discrete vapour-cavity model (DVCM), the discrete gas-cavity model (DGCM) by utilizing a low gas void fraction ($\alpha_g \leq 10^{-7}$) and the interface vaporous cavitation model ([2] and [5]). The discrete gas-cavity model is simple and performs accurately over a broad range of input parameters [13]. An improved DGCM that considers unsteady pipe friction is presented in this paper.

2 A DISCRETE GAS-CAVITY MODEL THAT CONSIDERS UNSTEADY FRICTION

The discrete gas-cavity model (DGCM) allows gas cavities to form at computational sections in the method of characteristics numerical grid. A liquid phase with a constant wave speed a is assumed to occupy the computational reach. The discrete gas-cavity model is described by the water-hammer compatibility equations (5) and (6), the continuity equation for the gas volume, and the ideal-gas equation [14]. Numerical forms of the continuity equation for the gas volume and the ideal gas equation within the staggered grid of the method of characteristics are:
- the continuity equation for the gas volume

$$\left(\forall_g\right)_{i,t} = \left(\forall_g\right)_{i,t-2\Delta t} + \left(\psi\left(\left(Q_d\right)_{i,t} - \left(Q_u\right)_{i,t}\right) + (1-\psi)\left(\left(Q_d\right)_{i,t-2\Delta t} - \left(Q_u\right)_{i,t-2\Delta t}\right)\right)2\Delta t \quad (8),$$

- plinska enačba

- the ideal-gas equation

$$\left(\forall_g\right)_{i,t} = \frac{\left(H_0 - z_0 - H_v\right)}{\left(H_{i,t} - z_i - H_v\right)}\alpha_{g0}A_i\Delta x \quad (9).$$

DPKM se uspešno uporablja za simuliranje plinske in parne ($\alpha_{g0} \leq 10^{-7}$) kavitacije. V slednjem primeru se izračun prostornine diskretne kavitacije po enačbi (9) ponovi, ko je izračunana prostornina po enačbi (8) negativna.

The DGCM model has been successfully used for the simulation of both gaseous and vaporous ($\alpha_{g0} \leq 10^{-7}$) cavitation. In the latter case, when the discrete cavity volume calculated by Eq. (8) is negative, then the cavity volume is recalculated by Equation (9).

2.1 Konvolucijski nestalni model trenja

Zielke [10] je s pomočjo analitičnih orodij razvil konvolucijski model (KM) nestalnega trenja za prehodni laminarni tok. Nestalni del koeficienta trenja v enačbi (7) popišemo kot konvolucijo utežne funkcije s krajevnimi pospeški v opazovanem časovnem pasu:

2.1 Convolution-Based Unsteady Friction Model

Zielke [10] analytically developed the convolution-based model (CBM) of unsteady friction for transient laminar flow. The unsteady part of the friction factor in Eq. (7) is defined by the convolution of a weighting function with past temporal accelerations:

$$f_u = \frac{32\nu A}{DQ|Q|}\int_0^t \frac{\partial Q}{\partial t^*}W_0\left(t - t^*\right)dt^* \quad (10).$$

Zielke je rešil enačbo (10) z upoštevanjem polne konvolucije, ki pa je računsko obsežna, saj obsega hitrosti v celotnem opazovanem časovnem pasu. Prispevek avtorjev k računsko učinkoviti in dovolj natančni rešitvi KM je v aproksimaciji utežne funkcije $W(\tau)$ kot končne vsote z N eksponentnimi členi [4]:

Zielke evaluated Eq. (10) using the full convolution scheme, which is computationally intensive because it requires convolution with a complete history of past velocities. The most recent approach to evaluate the CBM, which is efficient and accurate, makes an approximation of the weighting function $W(\tau)$ by a finite sum of N exponential terms [4]:

$$W_{app}\left(\tau\right) = \sum_{k=1}^{N} m_k e^{-n_k\tau} \quad (11).$$

Nestalni del koeficienta trenja je tedaj definiran kot:

The unsteady part of the friction factor is now defined as:

$$f_u = \frac{32\nu A}{DQ|Q|}\sum_{k=1}^{N} y_k\left(t\right) \quad (12),$$

kjer so členi $y_k(t)$ izraženi:

where the component $y_k(t)$ is expressed as follows:

$$y_k\left(t\right) = \int_0^t \frac{\partial Q}{\partial t^*}m_k e^{-n_k K\left(t-t^*\right)}dt^* \quad (13).$$

Pri tem konstanta K ($= 4\nu/D^2$) spremeni čas t v brezrazsežni čas $\tau = 4\nu t/D^2$. V času $t + 2\Delta t$ člen y_k izrazimo z enačbo:

And where the constant K ($= 4\nu/D^2$) converts the time t into the dimensionless time $\tau = 4\nu t/D^2$. At time $t + 2\Delta t$ the component y_k is:

$$y_k\left(t + 2\Delta t\right) = \int_0^{t+2\Delta t} \frac{\partial Q}{\partial t^*}m_k e^{-n_k K\left(t+2\Delta t-t^*\right)}dt^* \quad (14).$$

Rešitev gornjega integrala v obliki zapisa z brezrazsežnim časovnim korakom $\Delta\tau$ ($= K\Delta t$) da učinkovit vrnilni izraz za člen y_k in s tem tudi za f_u:

Solving the integral and writing it in terms of the dimensionless time step $\Delta\tau$ ($= K\Delta t$) finally gives an efficient recursive expression for the component y_k and hence for f_u:

$$y_k\left(t+2\Delta t\right)=e^{-n_k K\Delta t}\left\{e^{-n_k K\Delta t}y_k\left(t\right)+m_k\left[Q\left(t+2\Delta t\right)-Q\left(t\right)\right]\right\} \quad (15).$$

Člen $y_k(t)$ je izračunan v predhodnem časovnem koraku in je znan v času $t + 2\Delta t$. Tako ni treba izvajati konvolucije v celotnem opazovanem pasu. Izpeljali smo koeficiente eksponente vrste m_k in n_k za Zielkejevo utežno funkcijo za prehodni laminarni tok [10] in za Vardy-Brownove utežne funkcije za prehodni turbulentni tok ([11] in [12]), dobimo jih v [4].

CBM model nestalnega trenja ne napove rahlega faznega odmika tlaka, ki ga razberemo iz rezultatov meritev ([15] in [16]). Fazni odmik je posledica nizkofrekvenčnih komponent karakteristik prehodnega pojava, ki so običajno reda velikosti osnovne frekvence. Iz tega izhaja, da je dejanska hitrost širjenja valov rahlo nižja od napovedane. Kapljevina ima dodatno vztrajnost zaradi nestalne porazdelitve hitrosti po prerezu, ki jo popišemo z vztrajnostnim popravnim koeficientom β [16]. Vztrajnostni popravni koeficient (VPF) definiramo:

The component $y_k(t)$ was calculated during a previous time step and is known at time $t + 2\Delta t$. There is now no convolution with the complete history of velocities required. The coefficients of the exponential sum m_k and n_k were developed both for Zielke's weighting function for transient laminar flow [10] and for Vardy-Brown's weighting functions for transient turbulent flow ([11] and [12]) and can be found in [4].

The CBM of unsteady friction cannot produce the small low-frequency shift observed in experimental results ([15] and [16]). The low-frequency shift is related to the lowest-frequency components of the transient event, which are normally at the fundamental frequency. This suggests that the true wave speed is slightly lower than expected and the liquid has an extra inertia due to the velocity distribution, which is related to the momentum correction factor β[16]. The momentum correction factor (MCF) is defined as:

$$\beta=\frac{1}{AV^2}\int_A v^2 dA \quad (16).$$

Dejansko se β malo spreminja med prehodnim pojavom ([17] in [18]). Postavimo, da je koeficient β nespremenjen in sloni na začetnih pretočnih pogojih, tj. $\beta = \beta_0$. Obravnavni postopek je uporabljen tudi v podobnih primerih, kakor je izpeljava Vardy-Brownove utežne funkcije. VPF lahko določimo iz logaritmičnega ali potenčnega zakona porazdelitve hitrosti [19]. Uporabimo Reynoldsov transportni teorem, postavimo nespremenljivo vrednost VPF in dobimo gibalno enačbo, ki se razlikuje od enačbe (4):

Realistic values of β do not vary greatly during a transient event ([17] and [18]). It is assumed that β is constant and based on the steady conditions preceding the transient event, i.e., $\beta = \beta_0$. This is common to other analyses, such as the Vardy and Brown unsteady-friction weighting function. The MCF can be determined from either the log or power laws for the velocity distribution [19]. Using the Reynolds transport theorem, it can be shown that if the constant MCF is considered, then the equation of motion (4) becomes:

$$\frac{\partial H}{\partial x}+\frac{\beta_0}{gA}\frac{\partial Q}{\partial t}+f\frac{Q|Q|}{2gDA^2}=0 \quad (17).$$

Premena enačb (3) in (17) z metodo karakteristik da združljivostne enačbe vodnega udara, ki se v koračni obliki glase:

The finite-difference form of water-hammer compatibility equations obtained by the MOC transformation of Equations (3) and (17) is

- vzdolž C^+ karakteristike $\left(\Delta x/\Delta t=a/\sqrt{\beta_0}\right)$

- along the C^+ characteristic line $\left(\Delta x/\Delta t=a/\sqrt{\beta_0}\right)$

$$H_{i,t}-H_{i-1,t-\Delta t}+\frac{a\sqrt{\beta_0}}{gA}\left(\left(Q_u\right)_{i,t}-\left(Q_d\right)_{i-1,t-\Delta t}\right)+\frac{f\Delta x}{2gDA^2}\left(Q_u\right)_{i,t}\left|\left(Q_d\right)_{i-1,t-\Delta t}\right|=0 \quad (18),$$

- vzdolž C^- karakteristike $\left(\Delta x/\Delta t=-a/\sqrt{\beta_0}\right)$

- along the C^- characteristic line $\left(\Delta x/\Delta t=-a/\sqrt{\beta_0}\right)$

$$H_{i,t}-H_{i+1,t-\Delta t}-\frac{a\sqrt{\beta_0}}{gA}\left(\left(Q_d\right)_{i,t}-\left(Q_u\right)_{i+1,t-\Delta t}\right)-\frac{f\Delta x}{2gDA^2}\left(Q_d\right)_{i,t}\left|\left(Q_u\right)_{i+1,t-\Delta t}\right|=0 \quad (19).$$

Vpeljava β_0 v enačbe vodnega udara da manj strme karakteristike, ki upočasnijo potek prehodnega pojava.

The inclusion of β_0 in the water-hammer equations causes the slope of the characteristics to decrease, representing a slowing of the transient.

3 PREIZKUSNA POSTAJA

Preizkusna postaja za raziskave vodnega udara in kavitacijskega toka v ceveh je postavljena v Robinovem hidravličnem laboratoriju univerze v Adelaidi, Avstralija [20]. Merilna postaja je sestavljena iz ravnega bakrenega cevovoda z nagnjeno strmino dolžine 37,23 m (U_x = ± 0,01 m), notranjega premera 22,1 mm (U_x = ± 0,1 mm) in debeline stene cevi 1,63 mm (U_x = ± 0,05 mm). Cevovod je priključen na tlačni hram z leve in tlačni hram z desne strani (sl. 2). Merilna negotovost U_x je definirana kot kvadratni koren vsote kvadratov relativne in absolutne napake [21]. Strmina cevovoda je nagnjena s 5,45 % (U_x = ± 0,01 %).

Želeni tlak v obeh tlačnih hramih krmilimo z računalnikom. Neto prostornina vode v obeh tlačnih hramih in zmogljivost kompresorja omejujeta največjo stalno hitrost na 1,5 m/s in največji delovni tlak (tlačno višino) v obeh hramih na 400 kPa (40 m). Prehodni pojav na postaji je vzbujen s hitrim zapiranjem kroglastega zasuna. Hitro zaprtje ventila se lahko izvede z zapiralnim mehanizmom na torzijsko vzmet (čas zapiranja ventila t_c je nastavljiv od 5 do 10 milisekund) ali pa ročno. Vsak preizkus je izveden v dveh fazah. V prvi fazi dosežemo stalno pretočno hitrost (U_x = ± 1 % za prostorninsko metodo). V drugi fazi hitro zapiranje ventila vzbudi prehodni pojav. Hitrost širjenja udarnih valov (U_x = ± 0,1 %) je določena iz časa potovanja primarnega udarnega vala (prvi val, ki ga zazna tlačno zaznavalo) med zaprtim ventilom in bližnjo četrtino dolžine cevovoda.

3 EXPERIMENTAL APPARATUS

Laboratory apparatus for investigating water-hammer and column-separation events in pipelines was constructed in the Robin Hydraulics Laboratory at the University of Adelaide, Australia [20]. The apparatus comprises a straight 37.23 m (U_x = ±0.01 m) long sloping copper pipe of 22.1 mm (U_x = ±0.1 mm) internal diameter and of 1.63 mm (U_x = ±0.05 mm) wall thickness connecting two pressurized tanks (Fig. 2). The uncertainty in a measurement, U_x, is expressed as a root-sum-square combination of the bias and precision error [21]. The pipe slope is constant at 5.45% (U_x = ±0.01 %).

A specified pressure in each of the tanks is controlled by a computerized pressure-control system. The net water volume in both tanks and the capacity of the air compressor limits the maximum steady-state velocity to 1.5 m/s and the maximum operating pressure (pressure head) in each tank to 400 kPa (40 m). A transient event in the apparatus is initiated by a rapid closure of the ball valve. Fast closure of the valve is carried out either by a torsional spring actuator (the valve closure time t_c may be set from 5 to 10 milliseconds) or manually by hand. Each experiment using the apparatus consists of two phases. First, an initial steady-state velocity condition (U_x = ±1% for the volumetric method) is established. Second, a transient event is initiated by a rapid closure of the valve. The wave-propagation velocity (U_x = ±0.1%) is obtained from the measured time for the initial pressure wave (the first pressure wave passing the transducers) to travel between the closed valve and the quarter point nearest to the valve.

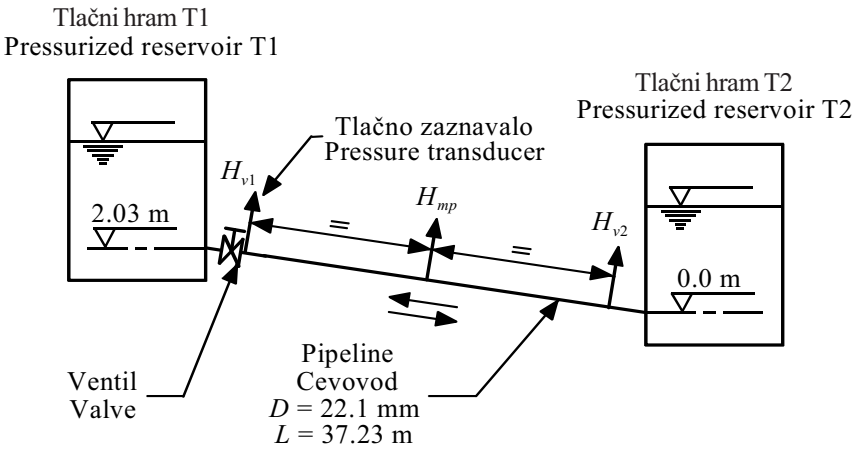

Sl. 2. *Preizkusna postaja*
Fig. 2. *Experimental apparatus layout*

Na navzgornjem in navzdolnjem koncu cevovoda ter na polovici dolžine cevovoda so na notranji premer cevi vgrajena piezoelektrična tlačna zaznavala (Kistler 610 B, $U_x = \pm 0{,}7$ %). Temperatura vode ($U_x = \pm$ 0,5 °C) je stalno merjena v hramu T1. Lega ventila med zapiranjem je merjena z optičnimi zaznavali ($U_x = \pm$ 0,0001 s). Meritev je registrirana in analizirana z merilnim računalnikom Concurrent 6655 v okolju UNIX.

4 PRIMERJAVA REZULTATOV IZRAČUNA IN MERITEV

Rezultati izračunov in meritev prehodnih pojavov v preizkusni postaji (sl. 2) so podani za dva primera z začetnima pretočnima hitrostima $V_0 = \{0{,}30; 1{,}40\}$ m/s pri stalni statični višini v tlačnem hramu T2 $H_{T2} = 22$ m [5]. Računski rezultati, dobljeni z DPKM z upoštevanjem nestalnega trenja po KM in vztrajnostnega popravnega koeficienta (DPKM + KM + VPF), so primerjani z rezultati meritev. Izračuni in meritve so bili izdelani za primer hitrega zapiranja ventila na navzdolnjem koncu cevovoda s pozitivno strmino pri tlačnem hramu T1 (sl. 2). Čas zapiranja ventila za oba primera je bil enak, $t_c = 0{,}009$ s, kar je precej krajše od odbojnega časa udarnega vala $2L/a = 2\times 37{,}23/1319 = 0{,}056$ s ($a = 1319$ m/s je izmerjena hitrost udarnega vala). Ventil začne hitro zapirati v času $t = 0{,}0$ s. V izračunu je izbran nabor števila cevnih odsekov $N = \{16, 32, 64, 128, 256\}$, da se preveri grobost računskega modela [22]. V enačbi (8) je bil izbran utežni koeficient $\psi = 1{,}0$, v enačbi (9) pa je bila izbrana dovolj majhna vrednost plinskega kavitacijskega razmernika $\alpha_{g0} = 10^{-7}$ ([13] in [14]). Vztrajnostni koeficient v enačbah (18) in (19) je odvisen od začetne pretočne hitrosti [19]; za $V_0 =$ 0,30 m/s znaša $\beta_0 = 1{,}0332$, za $V_0 = 1{,}40$ m/s pa $\beta_0 =$ 1,0224. Izdelali smo tudi izračune z DPKM z upoštevanjem navidezno stalnega modela trenja (DPKM+NST), da bi izluščili vpliv modelov trenja na rezultate izračuna. Izračunani in izmerjeni rezultati so primerjani pri ventilu (H_{v1}) in na polovici dolžine cevovoda (H_{mp}) (sl. 2).

Primerjava rezultatov izračuna in meritev za primer z začetno pretočno hitrostjo $V_0 = 0{,}30$ m/s in dveh števil računskih cevnih odsekov $N = \{32, 128\}$ je podana na slikah 3 in 4. Manjše število cevnih odsekov je običajno izbrano v inženirskih analizah vodnega udara. Večje število cevnih odsekov bi moralo dati bolj natančne rezultate izračuna (konvergenčni in stabilnostni kriterij).

Three flush-mounted piezoelectric-type pressure transducers (Kistler 610 B, $U_x = \pm 0.7$ %) are positioned at the endpoints and at the midpoint. The water temperature ($U_x = \pm 0.5$°C) in reservoir T1 is continuously monitored and the valve position during closure is measured using optical sensors ($U_x = \pm 0.0001$ s). Data acquisition and processing were performed with a Concurrent 6655 real-time UNIX data-acquisition computer.

4 COMPARISON OF COMPUTATIONAL AND EXPERIMENTAL RESULTS

A numerical and experimental analysis of the transient events in the laboratory apparatus (Fig. 2) is presented for two different initial flow-velocity cases $V_0 = \{0.30; 1.40\}$ m/s at a constant static head in the pressurized reservoir T2 $H_{T2} = 22$ m [5]. The numerical results from the DGCM and the CBM of unsteady friction with the momentum correction factor (DGCM+CBM+MCF) are compared with the results of measurements. Computational and experimental runs were performed for a rapid closure of the valve positioned at the downstream end of the upward sloping pipe at the pressurized tank T1 (Fig. 2). The valve closure time for the two runs was identical, $t_c = 0.009$ s, which is significantly shorter than the water-hammer wave-reflection time of $2L/a = 2\times 37.23/1319 = 0.056$ s ($a = 1319$ m/s is the measured water-hammer wave speed). The rapid valve closure begins at time $t = 0.0$ s. Different numbers of reaches were selected for each computational run $N = \{16, 32, 64, 128, 256\}$ to examine the numerical robustness of the model [22]. The value of the weighting factor $\psi = 1.0$ was used in Eq. (8), and a small gas void fraction of $\alpha_{g0} = 10^{-7}$ was selected in Eq. (9) ([13] and [14]). The momentum correction factor depends on the initial flow velocity [19] and its value used in Eqs. (18) and (19) is $\beta_0 = 1.0332$ for $V_0 = 0.30$ m/s and $\beta_0 =$ 1.0224 for $V_0 = 1.40$ m/s. In addition, the DGCM and the quasi-steady friction model (DGCM+QSF) results are included in the analysis to compare the effect of friction modelling on the computational results. The computational and experimental results are compared at the valve (H_{v1}) and at the midpoint (H_{mp}) (Fig. 2).

A comparison of the numerical and experimental results for an initial flow velocity $V_0 = 0.30$ m/s and different numbers of computational reaches $N = \{32, 128\}$ is presented in Figs. 3 and 4 respectively. Traditionally, a lower number of reaches is used in water-hammer analysis. A higher number of reaches should give more accurate results (convergence and stability criteria).

Hitro zapiranje ventila v primeru za H_{T2} = 22 m in začetno hitrost V_0 = 0,30 m/s vzbudi vodni udar s pretrganjem kapljevinskega stebra. Največjo izmerjeno višino pri ventilu $H_{v1;\,max}$ = 95,6 m razberemo po zrušitvi prve kavitacije v obliki ozkega tlačnega utripa. Obremenitev z največjo višino je kratkotrajna (0,00628 s). Največja izračunana višina z DPKM+NST je $H_{v1;\,max}$ = 99,6 m in z DPKM+KM+VPF $H_{v1;\,max}$ = 95,1m. Rezultati izračuna, dobljeni z DPKM+NST, se dobro ujemajo z izmerjenimi rezultati za prvi in drugi tlačni utrip. Odstopanja med rezultati se večajo s časom prehoda. Rezultati, dobljeni z DPKM+KM+VPF, se dobro ujemajo z izmerjenimi rezultati v širokem pasu opazovanja prehodnega pojava.

Primerjava rezultatov izračuna in meritev za primer z začetno pretočno hitrostjo V_0 = 1,40 m/s in dveh števil računskih cevnih odsekov N = {32, 128} je podana na slikah 5 in 6.

V obravnavanem primeru je največja višina pri ventilu enaka višini vodnega udara v času 2L/a po zaprtju ventila. Izmerjena največja višina je $H_{v1;\,max}$ = 210,9 m. Največji višini, določeni z DPKM+NST in DPKM+KM+VPF, se dobro ujemata

A rapid valve closure for H_{T2} = 22 m and an initial flow velocity V_0 = 0.30 m/s generates a water-hammer event with liquid column separation. The maximum measured head at the valve $H_{v1;\,max}$ = 95.6 m occurs as a short-duration pressure pulse after the first cavity collapses. The duration of the maximum head is very short (0.00628 s). The maximum computed heads predicted by DGCM+QSF and DGCM+CBM+MCF are $H_{v1;\,max}$ = 99.6 m and $H_{v1;\,max}$ = 95.1m, respectively. The computational results obtained by the DGCM+QSF agree well with the experimental results for the first and the second pressure-head pulse. The discrepancies between the results are greater for later times. The results obtained using the DGCM+CBM+MCF give pressure histories that are in good agreement with the experimental results for longer time periods.

A comparison of the numerical and experimental results for an initial flow velocity V_0 = 1.40 m/s and different numbers of computational reaches N = {32, 128} is presented in Figs. 5 and 6, respectively.

The maximum head at the valve for this case is the water-hammer head generated at a time of 2L/a after the valve closure. The value of the maximum measured head is $H_{v1;\,max}$ = 210.9 m. The maximum head predicted by the DGCM+QSF and

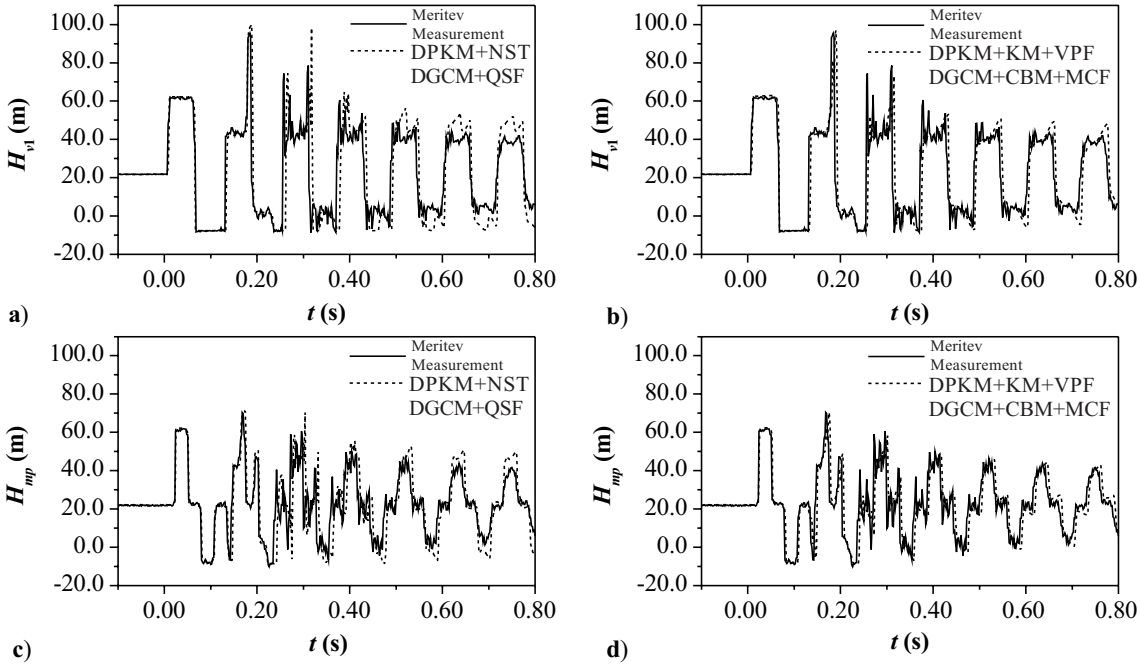

Sl. 3. *Primerjava višin pri ventilu (H_{v1}) in na polovici dolžine cevovoda (H_{mp}):*
Fig. 3. *Comparison of heads at the valve (H_{v1}) and at the midpoint (H_{mp}):*
V_0 = 0.30 m/s, H_{T2} = 22 m, N = 32

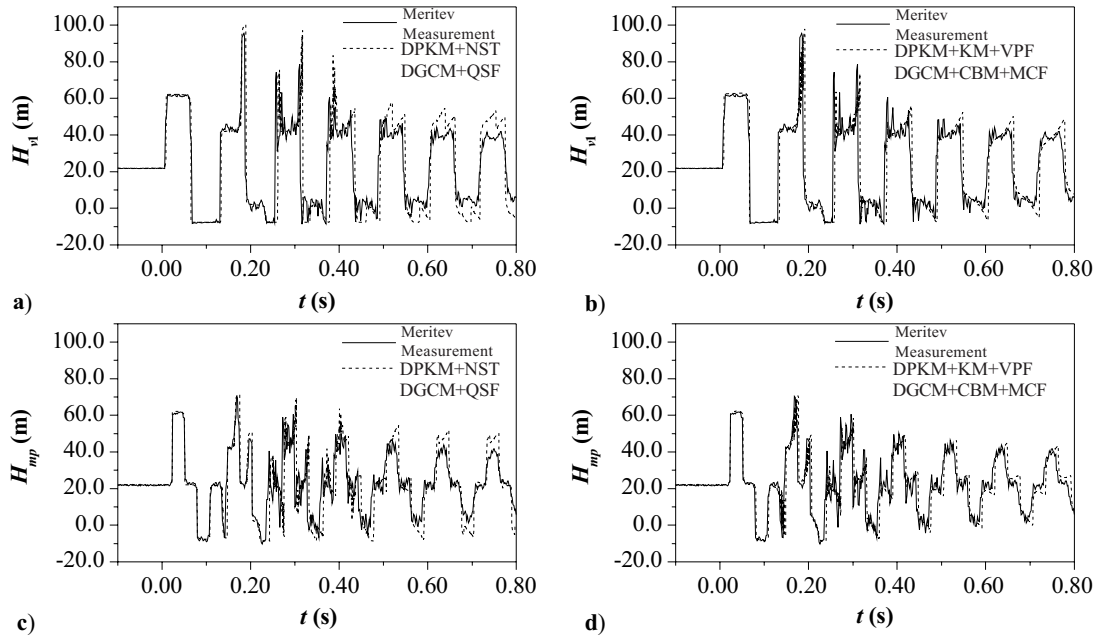

Sl. 4. *Primerjava višin pri ventilu (H_{v1}) in na polovici dolžine cevovoda (H_{mp}):*
Fig. 4. *Comparison of heads at the valve (H_{v1}) and at the midpoint (H_{mp}):*
$V_0 = 0.30$ m/s, $H_{T2} = 22$ m, $N = 128$

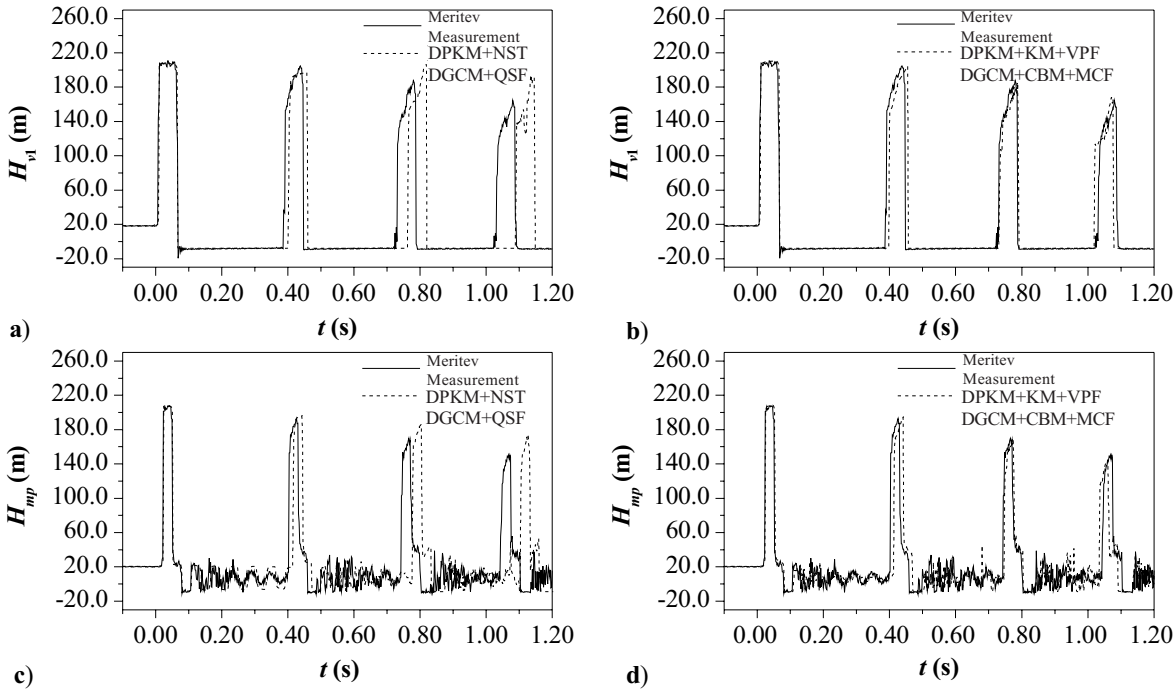

Sl. 5. *Primerjava višin pri ventilu (H_{v1}) in na polovici dolžine cevovoda (H_{mp}):*
Fig. 5. *Comparison of heads at the valve (H_{v1}) and at the midpoint (H_{mp}):*
$V_0 = 1.40$ m/s, $H_{T2} = 22$ m, $N = 32$

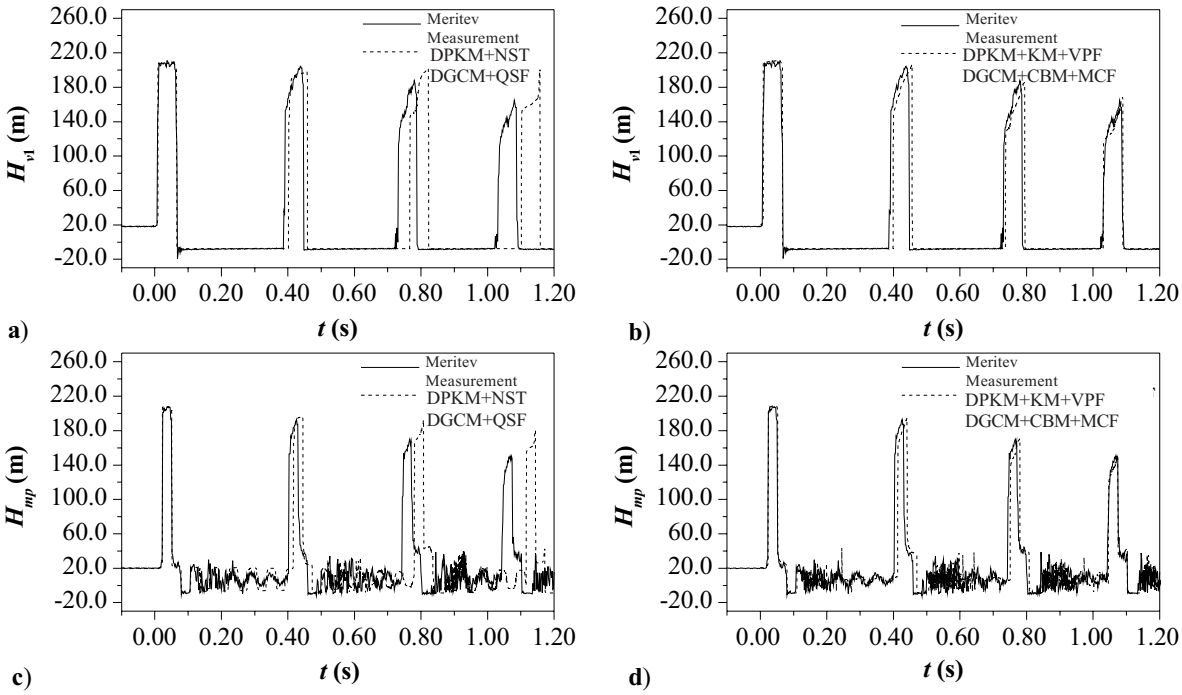

Sl. 6. *Primerjava višin pri ventilu (H_{v1}) in na polovici dolžine cevovoda (H_{mp}):*
Fig. 6. *Comparison of heads at the valve (H_{v1}) and at the midpoint (H_{mp}):*
$V_0 = 1.40$ m/s, $H_{T2} = 22$ m, N = 128

z izmerjeno višino. Čas obstoja prve kavitacije pri ventilu, določen z DPKM+KM+VPF, se bolje ujema od časa, določenega z DPKM+NST (meritev: 0,318 s; DPKM+NST: 0,331 s; DPKM+KM+VPF: 0,325 s). Rezultati izračuna, dobljeni z DPKM+NST, se dobro ujemajo z rezultati meritve do zrušitve prve kavitacije pri ventilu. Iz rezultatov, dobljenih z DPKM+KM+VPF, razberemo znatno izboljšanje napovedi dušenja in faznega odmika tlačnih utripov v primerjavi z rezultati, dobljenimi z DPKM+NST. Rezultati izračuna z večjim številom cevnih odsekov se bolje ujemajo z rezultati meritev. Sklepamo, da upoštevanje modela nestalnega trenja v DPKM (DPKM+KM+VPF) da bolj natančne rezultate v primerjavi z rezultati, dobljenimi z upoštevanjem modela navidezno stalnega trenja (DPKM+NST).

4.1 Konvergenca in stabilnost

Numerični model DPKM+KM+VPF, vgrajen v MK računsko mrežo, mora zadostiti konvergenčnim in stabilnostnim kriterijem. Konvergenca definira stalno rešitev, ko se Δx in

DGCM+CBM+MCF closely matches the measured head. The duration of the first cavity at the valve is predicted better by the DGCM+CBM+MCF than by the DGCM+QSF (measurement: 0.318 s; DGCM+QSF: 0.331 s; DGCM+CBM+MCF: 0.325 s). Computational results obtained with the DGCM+QSF agree well with experimental results until the first cavity at the valve collapses. The results from the DGCM+CBM+MCF show significant improvement in terms of both the attenuation and phase shift of the pressure-head traces when compared to the DGCM+QSF results. When the number of computational reaches is increased, the computational and measured results agree better. Inclusion of the unsteady-friction model into the DGCM (DGCM+CBM+MCF) significantly improves the results compared to those using the quasi-steady friction model (DGCM+QSF).

4.1 Convergence and Stability

The numerical solution of the DGCM+CBM+MCF incorporated into the MOC computational grid should satisfy the convergence and stability criteria. Convergence relates to the behaviour of

Δt približujeta ničli, stabilnost rešitve pa je odvisna od napake zaokrožitve [1]. V tem prispevku sta konvergenca in stabilnost DPKM+KM+VP in DPKM+NST preverjena z metodo nabora cevnih odsekov [22] v pasu $N = \{16, 32, 64, 128, 256\}$. Na sliki 7 so podani rezultati izračuna za primer z

the solution as Δx and Δt tends to zero, while stability is concerned with the round-off error growth [1]. The influence of the different numbers of computational reaches $N = \{16, 32, 64, 128, 256\}$ is investigated for the DGCM+CBM+MCF [22]. In addition, a numerical analysis of the DGCM+QSF model is included as well. Fig. 7

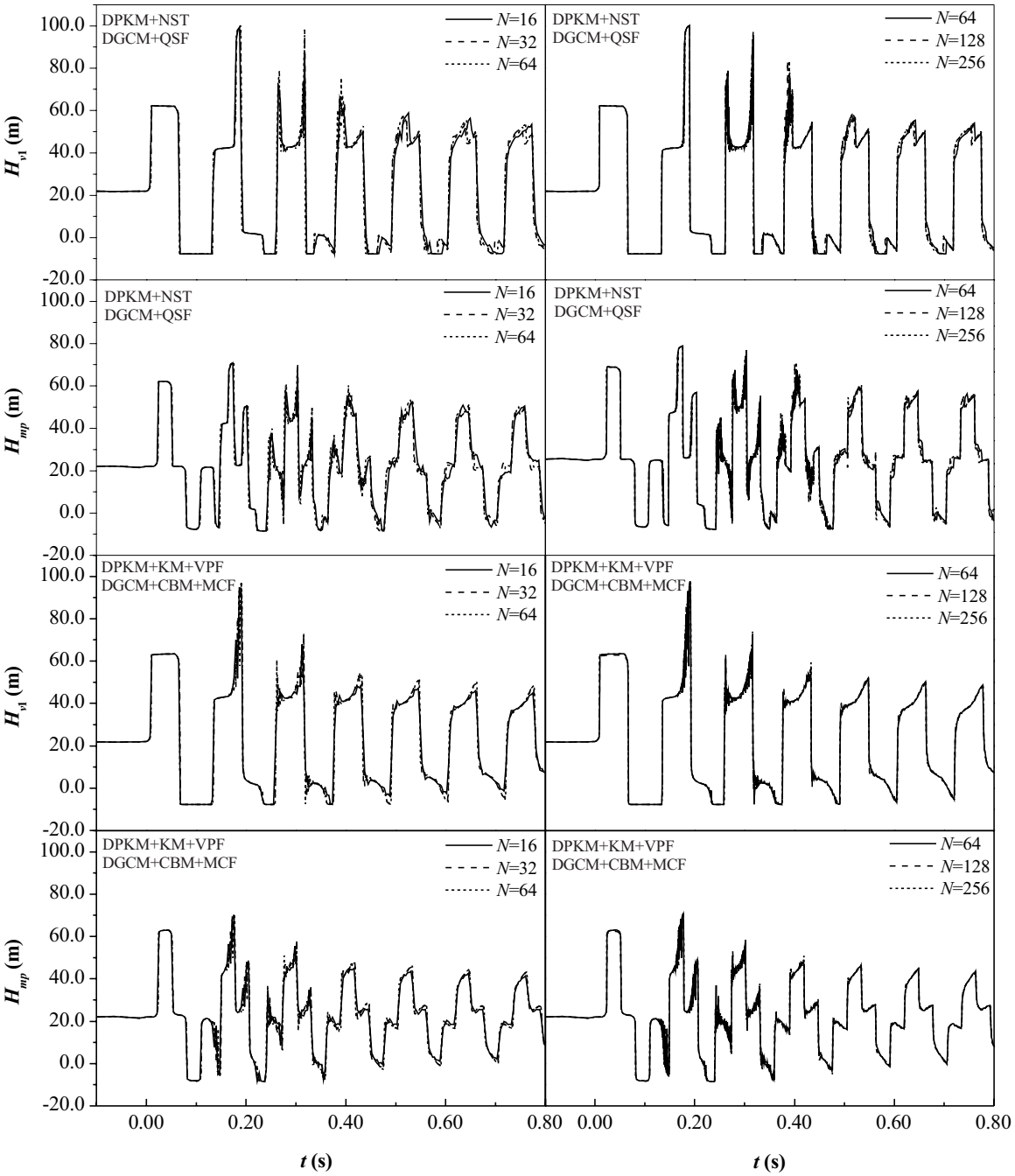

Sl. 7. *Računska analiza:* $V_0 = 0{,}30$ *m/s,* $H_{T2} = 22$ *m*

Fig. 7. *Numerical analysis:* $V_0 = 0.30$ *m/s,* $H_{T2} = 22$ *m*

začetno pretočno hitrostjo V_0 = 0,30 m/s z blago kavitacijo. Rezultati, dobljeni z obema modeloma so konzistentni s povečanjem števila odsekov. To pa ne velja za rezultate izračuna v primeru z začetno hitrostjo V_0 = 1,40 m/s na sliki 8. Intenzivna kavitacija vzdolž cevi v obliki področij

shows the numerical results for the case with an initial flow velocity V_0 = 0.30 m/s with moderate cavitation. The results for both models are consistent as the number of reaches is increased. This is not the case for the numerical runs with initial velocity V_0 = 1.40 m/s in Fig. 8. Severe cavitation along the pipeline forms distributed,

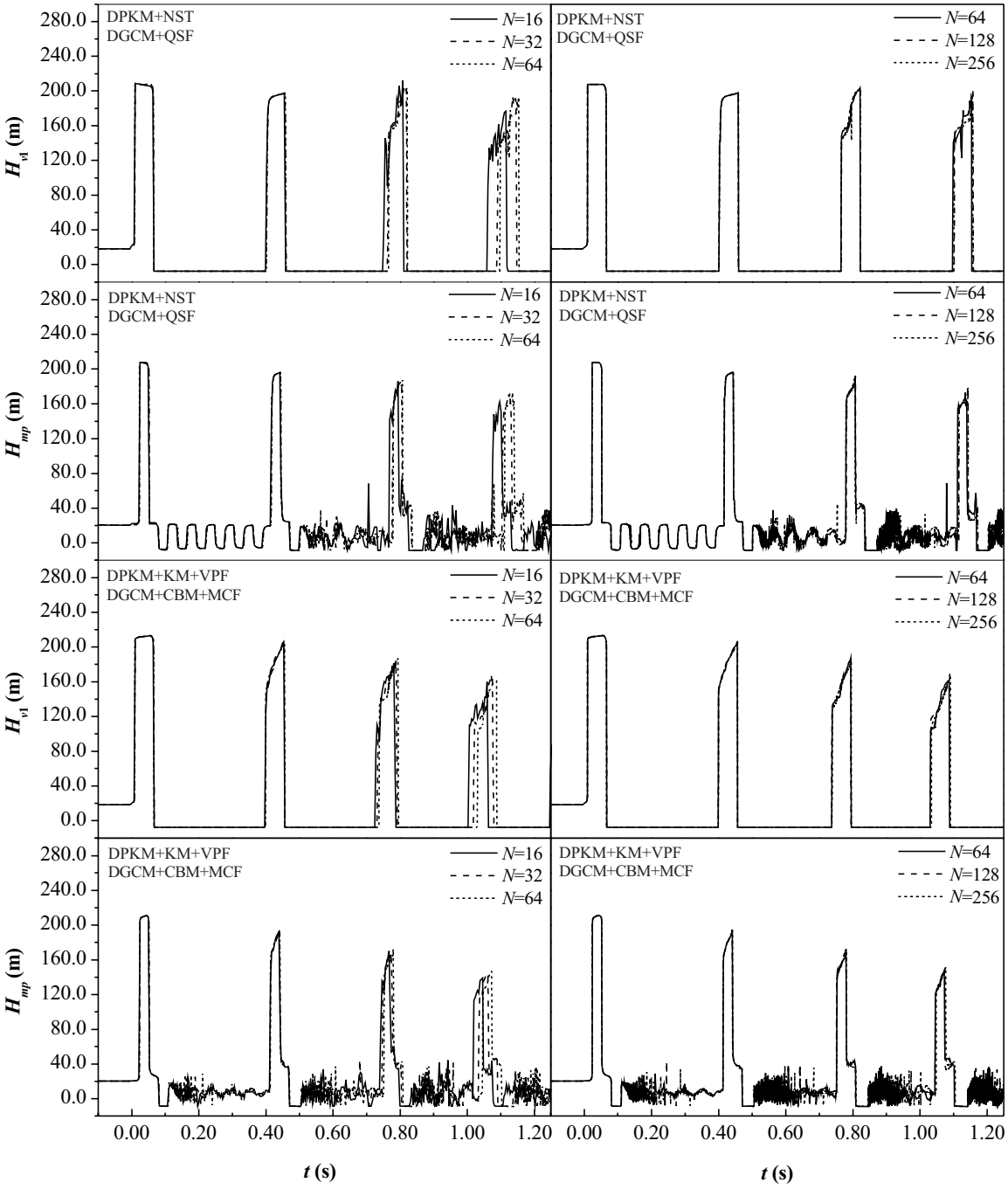

Sl. 8. *Računska analiza: V_0 = 1,40 m/s, H_{T2} = 22 m*
Fig. 8. *Numerical analysis: V_0 = 1.40 m/s, H_{T2} = 22 m*

nepretrganega parnega kavitacijskega toka in diskretnih kavitacij, ki jih razberemo iz meritev, je v DPKM modelih (sl. 5 in 6) popisana približno. Zrušitev velike kavitacije pri ventilu in diskretnih kavitacij vzdolž cevovoda vzbudi strma tlačna valovna čela, ki potujejo vzdolž cevi. Primerjava rezultatov izračuna in meritev (sl. 5 in 6) jasno pokaže, da DPKM+KM+VPF bolje popiše fizikalni pojav pri večjem številu cevnih odsekov. V splošnem amplituda in časovni potek glavnih tlačnih utripov, določenih z upoštevanjem navidezno stalnega in nestalnega trenja, konvergirata s povečanjem števila cevnih odsekov (vsak model konvergira k nekoliko različnemu rezultatu). DPKMne vzbudi visokih fizikalno nerealnih tlačnih utripov v primerjavi z diskretnim parnim kavitacijskim modelom (DPAKM) ([7] in [13]). Računska modela pa ne napovesta nekaterih visokofrekvenčnih utripov, razbranih v meritvah. Dosedanje preizkusne raziskave so pokazale, da prehodne kavitacije vzdolž cevi niso homogene ([23] in [24]), zato nekateri visokofrekvenčni pulzi niso ponovljivi in tudi ne vplivajo na glavne tlačne utripe. Podoben pojav lahko izluščimo v rezultatih izračuna z DPKM, pri katerih so nekateri visokofrekvenčni tlačni utripi vplivani s številom cevnih odsekov. Ta pojav zaznamo v področjih z blago kavitacijo vzdolž cevovoda (nepretrgani parni kavitacijski tok, diskretne kavitacije) kot posledico popisa kavitacije z različnim številom cevnih odsekov. Ta vpliv pa je zanemarljiv v primerjavi z odzivom na veliki skali.

5 SKLEP

Podana je primerjava med rezultati izračuna in meritev za primer hitrega zapiranja navzdolnjega ventila v preprostem cevnem sistemu. Primerjana sta diskretni plinski kavitacijski model z upoštevanjem navidezno stalnega kapljevinskega trenja (DPKM+NST) in nestalnega trenja z uporabo konvolucijega modela (DPKM+KM+VPF). Primerjalna analiza obsega primer z blago in primer z intenzivno kavitacijo. Konvolucijski model nestalnega trenja bolj natančno popiše nestalno kapljevinsko trenje v primerjavi z navidezno stalnim približkom. Upoštevanje nestalnega trenja v DPKM da zato bolj natančne računske rezultate. Raziskali smo tudi vpliv izbire števila cevnih odsekov. Računska analiza pokaže, da je DPKM+KM+VPF grob s povečanjem števila cevnih

vaporous cavitation zones and intermediate cavities that have been recorded by measurements and only approximately accounted for in the DGCMs (Figs. 5 and 6). The collapse of a large cavity at the valve and intermediate cavities along the pipe create steep pressure wave fronts that travel along the pipe. Comparisons between the measured and computed results clearly showed (Figs. 5 and 6) that the DGCM+CBM+MCF better represents the real flow situation as the number of computational reaches is increased. Generally, the magnitude and timing of the main pressure pulses predicted by the DGCM model using either the quasi-steady or the convolution-based model converge as the number of reaches is increased (although each method converges to a slightly different solution). The DGCM model does not generate large, unrealistic pressure spikes in comparison to the discrete vapour-cavity model (DVCM) ([7] and [13]). However, there still remain some high-frequency peaks in the experimental measurements that are not reproduced by either numerical model. Previous experimental studies clearly showed that transient cavities along the pipeline are not distributed homogeneously ([23] and [24]); therefore, some high-frequency peaks are not repeatable and do not affect the main pressure pulses significantly. A similar behaviour is revealed in the DGCM computational results in that some high-frequency peaks vary with the different numbers of reaches. This behaviour occurs in regions with distributed vaporous cavitation and intermediate cavities where small-scale cavitation takes place in slightly different ways for different numbers of computational reaches. However, typically this behaviour is small compared to the bulk transient response.

5 CONCLUSION

Results from the discrete gas-cavity model with the quasi-steady friction approximation (DGCM+QSF) and with the convolution-based unsteady-friction model (DGCM+CBM+MCF) are compared with the results of measurements for a fast-downstream end-valve closure in a simple reservoir-pipeline-valve laboratory apparatus. A comparative analysis includes experimental tests for two different flow conditions with moderate and severe cavitation. The convolution-based unsteady-friction model better captures the behaviour of unsteady fluid friction than the quasi-steady friction approximation. The results clearly show that the inclusion of unsteady friction into the DGCM significantly improves the numerical results. The influence of the different numbers of reaches is also investigated. The examination of the computational results reveals the numerically robust

odsekov. Obravnavani model zaradi dobrega ujemanja rezultatov izračuna z meritvami in računske grobosti priporočamo za inženirsko uporabo.

behaviour of the DGCM+CBM+MCF as the number of reaches increases. Due to the excellent matches with experimental data and the robust numerical algorithm this model is recommended for engineering practice.

Zahvala

Ta prispevek je bil napisan med obiskom gospoda Karadžića v Litostroju E.I. d.o.o. od 5. januarja do 28. februarja 2005. Avtorji se toplo zahvaljujejo Litostroju in CMEPIUSu (Center za mobilnost in evropske programe izobraževanja in usposabljanja) za podporo tega obiska. Za podporo raziskav se toplo zahvaljujejo tudi ARRSu (Agencija za raziskovalno dejavnost Republike Slovenije).

Acknowlegments

This paper was written during Mr Karadžić's visit to Litostroj E.I. d.o.o. from January 5 to February 28, 2005. The authors wish to thanks Litostroj and CMEPIUS (Centre of the Republic of Slovenia for Mobility and European Programmes for Education and Training) who supported this visit. The support of the research by ARRS (Slovenian Research Agency) is gratefully acknowledged as well.

6 OZNAČBE
6 SYMBOLS

prečni prerez	A	pipe area
hitrost širjenja udarnih (tlačnih) valov	a	water-hammer (pressure) wave speed
premer cevi	D	pipe diameter
Darcy-Weisbachov koeficient trenja	f	Darcy-Weisbach friction factor
zemeljski pospešek	g	gravitational acceleration
piezometrična višina (višina)	H	piezometric head (head)
parna tlačna višina	H_v	gauge vapour pressure head
dolžina cevi	L	pipe length
koeficienti eksponentne vrste	m_k, n_k	exponential sum coefficients
število cevnih odsekov	N	number of computational reaches
pretok	Q	discharge
navzdolnji pretok	Q_d	node downstream end discharge
navzgornji pretok	Q_u	node upstream end discharge
Reynoldsovo število = VD/ν	R_e	Reynolds number = VD/ν
čas	t, t^*	time
čas zapiranja ventila	t_c	valve closure time
merilna negotovost	U_x	uncertainty in a measurement
povprečna pretočna hitrost	V	average flow velocity
pretočna hitrost	v	flow velocity
utežna funkcija	W	weighting function
kordinata vzdolž cevi	x	distance along the pipe
člen utežne funkcije	y_k	component of the weighting function
geodetska višina	z	pipeline elevation
plinski kavitacijski razmernik	α_g	gas void fraction
vztrajnostni korekcijski koeficient	β	momentum correction factor
časovni korak	Δt	time step
dolžina cevnega odseka	Δx	reach length
brezrazsežni časovni korak	$\Delta \tau$	dimensionless time step
strmina cevovoda	θ	pipe slope
kinematična viskoznost	ν	kinematic viscosity
brezrazsežni čas	τ	dimensionless time
utežni koeficient	ψ	weighting factor
diskretna prostornina kavitacije	$\forall$	discrete cavity volume

Indeksi:		*Subscripts:*
približen	*app*	approximate
plin	*g*	gas
računska točka	*i*	node number
polovica dolžine cevovoda	*mp*	midpoint
navidezno stalni del	*q*	quasi-steady part
hram	T	tank (reservoir)
čas	*t*	time
nestalni del	*u*	unsteady part
ventil	*v*	valve
stalen (začeten) ali referenčen	0	steady state (initial) or reference

Okrajšave:		*Abbreviations:*
diskretni plinski kavitacijski model	DPKM/DGCM	discrete gas-cavity model
diskretni plinski kavitacijski model z navidezno stalnim trenjem	DPKM+NST/ DGCM+QSF	discrete gas-cavity model with quasi-steady friction
diskretni plinski kavitacijski model s konvolucijskim modelom in vztrajnostnim popravnim faktorjem	DPKM+KM+ +VPF/DGCM+ +CBM+MCF	discrete gas-cavity model with convolution-based model and momentum correction factor
diskretni parni kavitacijski model	DPAKM/DVCM	discrete vapour-cavity model
metoda karakteristik	MK/MOC	method of characteristics

7 LITERATURA
7 REFERENCES

[1] Chaudhry, M.H. (1987) Applied hydraulic transients. *Van Nostrand Reinhold Company,* New York, ZDA.

[2] Wylie, E.B., Streeter, V.L. (1993) Fluid transients in systems. *Prentice Hall*, Englewood Cliffs, ZDA.

[3] Bergant, A., Tijsseling, A. (2001) Parameters affecting water hammer wave attenuation, shape and timing. *Proceedings of the 10th International Meeting of the IAHR Work Group on the Behaviour of Hydraulic Machinery under Steady Oscillatory Conditions*, Trondheim, Norveška, Prispevek C2, 12 strani.

[4] Vítkovský, J., Stephens, M., Bergant, A., Lambert, M., Simpson, A.R. (2004) Efficient and accurate calculation of Zielke and Vardy-Brown unsteady friction in pipe transients. *Proceedings of the 9th International Conference on Pressure Surges*, BHR Group, Chester, Velika Britanija, 15 strani.

[5] Bergant A., Simpson, A.R. (1999) Pipeline column separation flow regimes. *Journal of Hydraulic Engineering*, ASCE,125(8), 835 - 848.

[6] Golia, U.M. (1990) Sulla valutazione delle forze resistenti nel colpo d'ariete. *Report No.639, Department of Hydraulic and Environmental Engineering*, *University of Naples*, Naples, Italija (v italjanščini).

[7] Bergant A., Simpson, A.R. (1994) Estimating unsteady friction in transient cavitating pipe flow. *Proceedings of the 2nd International Conference on Water Pipeline Systems*, BHR Group, Edinburgh, Velika Britanija, 333 - 342.

[8] Bergant, A., Simpson, A.R., Vítkovský, J. (2001) Developments in unsteady pipe flow friction modeling. *Journal of Hydraulic Research*, IAHR, 39(3), 249 - 257.

[9] Vardy, A.E. (1980) Unsteady flow: fact and friction. *Proceedings of the 3rd International Conference on Pressure Surges*, BHRA, Cantenbury, Velika Britanija, 15 - 26.

[10] Zielke, W. (1968) Frequency-dependent friction in transient pipe flow. *Journal of Basic Engineering*, ASME, 90(1), 109 - 115.

[11] Vardy, A.E., Brown, J.M.B. (2003) Transient turbulent friction in smooth pipe flows. *Journal of Sound and Vibration*, 259(5), 1011 - 1036.

[12] Vardy, A.E., Brown, J.M.B. (2004) Transient turbulent friction in fully rough pipe flows. *Journal of Sound and Vibration*, 270, 233 - 257.

[13] Simpson, A.R., Bergant, A. (1994) Numerical comparison of pipe-column-separation models. *Journal of Hydraulic Engineering*, ASCE, 120(3), 361 - 377.
[14] Wylie, E. B. (1984) Simulation of vaporous and gaseous cavitation. *Journal of Fluids Engineering*, ASME, 106(3), 307 - 311.
[15] Brown, F.T., Margolis, D.L., Shah, R.P. (1969) Small-amplitude frequency behavior of fluid lines with turbulent flow. *Journal of Basic Engineering*, ASME, 91(4), 678 - 693.
[16] Bergant, A., Tijsseling, A., Vítkovský, J., Covas, D., Simpson, A.R., Lambert, M. (2003) Further investigations of parameters affecting water hammer wave attenuation, shape and timing. Part 1: Mathematical tools. *Proceedings of the 11th International Meeting of the IAHR Work Group on the Behaviour of Hydraulic Machinery under Steady Oscillatory Conditions*, Stuttgart, Nemčija, 12 strani.
[17] Buthaud, H. (1977) On the momentum correction factor in pulsatile blood flow. *Journal of Applied Mechanics*, ASME, 44(2), 343 - 344.
[18] Brunone, B., Golia, M.U., Greco, M. (1991) Some remarks on the momentum equation for fast transients. *International Meeting on Hydraulic Transients with Column Separation*, *9th Round Table*, IAHR, Valencia, Španija, 140 - 148.
[19] Chen, C.L. (1992) Momentum and energy coefficients based on power-law velocity profile. *Journal of Hydraulic Engineering*, ASCE, 118(11), 1571 - 1584.
[20] Bergant, A., Simpson, A.R. (1995) Water hammer and column separation measurements in an experimental apparatus. *Research Report No. R128*, Department of Civil and Environmental Engineering, University of Adelaide, Adelaide, Avstralija.
[21] Coleman, H.W., Steele, W.G. (1989) Experimentation and uncertainty analysis for engineers. *John Wiley and Sons*, New York, ZDA.
[22] Maudsley, D. (1984) Errors in simulation of pressure transients in a hydraulic system. *Proceedings of the Institute of Measurement and Control*, 6(1), 7 - 12.
[23] Fan, D., Tijsseling, A. (1992) Fluid-structure interaction with cavitation in transient pipe flows. *Journal of Fluids Engineering*, ASME, 114(2), 268 - 274.
[24] Simpson, A.R., Bergant, A. (1996) Interesting lessons from column separation experiments. *Proceedings of the 7th International Conference on Pressure Surges*, BHR Group, Harrogate, Velika Britanija, 83 - 97.

Naslovi avtorjev: doc.dr. Anton Bergant
Litostroj E.I. d.o.o.
Litostrojska 50
1000 Ljubljana
anton.bergant@litostroj-ei.si

mag. Uroš Karadžić
Univerzitet Crne Gore
Mašinski fakultet
Cetinjski put b.b.
81000 Podgorica
Srbija i Crna Gora
urosk@cg.ac.yu

dr. John P. Vítkovský
Oddelek za naravne vire in
rudarstvo
Indooroopilly, QLD 4068
Avstralija
john.vitkovsky@nrm.qld.gov.au

Authors' Addresses: Doc.Dr. Anton Bergant
Litostroj E.I. d.o.o.
Litostrojska 50
1000 Ljubljana, Slovenia
anton.bergant@litostroj-ei.si

Mag. Uroš Karadžić
University of Montenegro
Faculty of Mechanical Engineering
Cetinjski put n.n.
81000 Podgorica
Serbia and Montenegro
urosk@cg.ac.yu

Dr. John P. Vítkovský
Department of Natural
Resources & Mines
Indooroopilly, QLD 4068
Australia
john.vitkovsky@nrm.qld.gov.au

dr. Igor Vušanović
Univerzitet Crne Gore
Mašinski fakultet
Cetinjski put b.b.
81000 Podgorica
Srbija i Crna Gora
igorvus@cg.ac.yu

prof. Angus R. Simpson
Šola gradbenega in okoljskega
inženirstva
Univerza v Adelaidi
Adelaide, SA 5005
Avstralija
asimpson@civeng.adelaide.edu.au

Dr. Igor Vušanović
University of Montenegro
Faculty of Mechanical Engineering
Cetinjski put n.n.
81000 Podgorica
Serbia and Montenegro
igorvus@cg.ac.yu

Prof. Angus R. Simpson
School of Civil & Environmental
Engineering
University of Adelaide
Adelaide, SA 5005
Australia
asimpson@civeng.adelaide.edu.au

Prejeto: 18.2.2005
Received:

Sprejeto: 29.6.2005
Accepted:

Odprto za diskusijo: 1 leto
Open for discussion: 1 year